

---

# Fabrication Limits of Electron Beam Lithography and of UV, X-Ray and Ion-Beam Lithographies

Alec N. Broers

*Phil. Trans. R. Soc. Lond. A* 1995 **353**, 291-311

doi: 10.1098/rsta.1995.0101

---

## Email alerting service

Receive free email alerts when new articles cite this article - sign up in the box at the top right-hand corner of the article or click [here](#)

---

To subscribe to *Phil. Trans. R. Soc. Lond. A* go to:  
<http://rsta.royalsocietypublishing.org/subscriptions>

---

# Fabrication limits of electron beam lithography and of UV, X-ray and ion-beam lithographies

BY ALEC N. BROERS

*Churchill College, Cambridge CB3 0DS, UK, and Department of Engineering,  
University of Cambridge, Trumpington Street, Cambridge CB2 1PZ, UK*

The paper discusses and compares the lithography methods being developed for the fabrication of future generations of silicon integrated circuits. The smallest features in today's circuits are about  $0.3\ \mu\text{m}$  in size and this will be reduced to  $0.1\ \mu\text{m}$  within the next ten years. The methods discussed include optical (ultraviolet light) projection, which is used predominantly at present, projection printing at wavelengths between the X-ray and ultraviolet regions, X-ray proximity printing, and scanning and projection with electrons and ions. There are severe problems to be overcome with all of the methods before they can satisfy future needs. The difficulties are not just connected with obtaining adequate resolution. The more challenging requirements are those associated with the elimination of distortion in the highly complex trillion pixel images and of achieving an exposure rate of about one per second with a system of acceptable cost, that is less than about \$10M. The various approaches for correcting distortion and obtaining adequate throughput are described, as are the factors limiting resolution. Finally, the ultimate capabilities of electron beam methods for fabricating structures and devices with dimensions down to 1 nm are described.

## 1. Introduction

This paper addresses two aspects of electron-beam lithography: first, its capabilities in comparison with other methods for fabricating microelectronic integrated circuits and second, its resolution limits for fabricating nanostructures. In the first case, its writing speed is not high enough for the manufacturing of today's highly complex chips, but it can be used for making custom devices and masks. In the second case, its ultimate resolution is set by the fabrication process and not by the electron optics.

## 2. Integrated circuit fabrication

### (a) *Device and circuit requirements*

It has become clear that the benefits of miniaturizing conventional semiconductor devices will continue, at least until dimensions reach  $0.05\ \mu\text{m}$ , that is until they are about ten times smaller than they are today.  $0.05\ \mu\text{m}$  is beyond the resolution of the ultraviolet (UV) projection cameras presently used to expose the patterns for these circuits, so a replacement will have to be found if these sub- $0.1\ \mu\text{m}$  devices are to be commercially viable. Finding a replacement will be a formidable task, not

*Phil. Trans. R. Soc. Lond. A* (1995) **353**, 291–311

*Printed in Great Britain*

291

© 1995 The Royal Society

T<sub>E</sub>X Paper

because of the need for higher resolution, but because microcircuit images contain an astronomically large number of pixels. There are more pixels in an integrated circuit image than in any other type of image, except perhaps an aerial photograph. For example, the image for a 1 Gbit memory chip, to be produced by the year 2000, will contain about  $250\,000 \times 750\,000 = 1.9 \times 10^{11}$  pixels, which is the same as that contained in 500 000 TV images. The diameter of a pixel is defined here as one quarter of the minimum feature size.

To add to the difficulty, there is the unique requirement that the images must be completely distortion free so that the different layers of the microcircuit precisely overlay each other. There may be more than twenty of these. In addition, each image must be printed in a few seconds by a system of acceptable cost. It has been the reduction in cost per circuit that has led to the proliferation of integrated circuits, so it is pointless to reduce the size of the devices further unless this leads to a further reduction in cost.

At present, the only obvious way to achieve the immense pixel throughput is to use a system in which the image of the chip, or at least a large fraction of the image, is printed in parallel. Such systems are known as 'replication' systems because they replicate a mask. The mask can be written at a slower pace by a scanning-beam system. 'Direct writing' on the silicon wafer with a scanning beam is not feasible because it is too slow. The fastest scanning systems, which are the variable shaped electron-beam systems, only run today at a maximum exposure rate of around 109 pixels per second, so they would take about 200 s to write the pattern for one level of a 1 Gbit chip. This is more than 100 times longer than it would take a UV replication camera. The cost of a scanning electron-beam system is \$10M to \$15M which is typically five times that of an optical camera, so it is clear that direct-writing is not cost competitive.

In this paper the various lithography methods being developed for integrated circuit lithography are briefly described and their ultimate capabilities compared. The patterning capability of electron-beam methods are then discussed in more detail.

### (b) *UV light projection*

Since the earliest days when contact or proximity printing was used, UV light projection has been used for the mass production of integrated circuits. It is not possible to forecast accurately the resolution limit of this method but the ultimate UV camera is likely to operate at a wavelength ( $\lambda$ ) of about 160 nm and have a lens with a numerical aperture (NA) of about 0.75. It can be estimated, using the standard expression for the minimum feature size,  $k\lambda/\text{NA}$ , where  $k$  is typically 0.8, that the camera would reproduce 0.17  $\mu\text{m}$  lines.  $k$  depends on the mask type, the illumination and the contrast required by the resist process. With phase-shift masks and off-axis illumination, as described for example by Okazaki (1991), and a resist in which only a shallow surface layer needs to be exposed (Coopmans & Roland 1987; de Beeck & Van den Hove 1992), a value for  $k$  of 0.5 might be reached and the feature size reduced to 0.1  $\mu\text{m}$ . This would allow the 1 Gbit chip and its equivalents to be made with UV projection and perhaps the next generation of chips as well. The problem is that the depth of focus, as given by  $\lambda/(\text{NA})^2$ , would fall to 0.28  $\mu\text{m}$ , which many would regard as impractical, but it may be possible to increase the effective depth of focus by new methods such as the use of dual masks spaced along the optical axis.

Small depth of focus is not the only problem to be overcome before this ultimate UV system will become practicable, however. Difficulties remain with sources

and with the fabrication of optical components for the sub-200 nm region. Of these, densification and colour centre formation in fused quartz, and the lack of suitably reliable laser sources, have already been identified. The performance of lasers in the vacuum UV regime will also have to be improved.

Overall, 0.1  $\mu\text{m}$  would seem to be a reasonable ultimate limit for UV lithography.

(c) *Soft X-ray projection and X-ray lithography*

To go beyond 0.1  $\mu\text{m}$  linewidth, UV light will have to be abandoned and shorter wavelength radiation used. There are severe difficulties with the fabrication of focusing elements in the very soft X-ray regime, but significant progress has been made with multi-layer mirrors for about 13 nm radiation and this has led to proposals for the use of projection imaging at soft X-ray wavelengths for integrated circuit lithography (Tennant *et al.* 1991; Kurihara *et al.* 1991; White 1991). Others argue that it will be impossible to meet the 1 nm tolerances that are needed on the mirror surfaces to meet image distortion requirements and that it will be better to reduce the wavelength even further, that is down to 0.5–2 nm, and simply form the image by shadow printing (Spears & Smith 1972; Smith & Schattenburg 1992). Shadow printing, which is known as X-ray lithography, has received considerably more attention than projection imaging.

In manufacturing, mask and wafer must be separated if they are not to damage each other and the limiting resolution of X-ray lithography is about 0.07  $\mu\text{m}$ , as set by Fresnel diffraction between the mask and the wafer. The minimum linewidth is approximately given by the simple expression  $\sqrt{\lambda g}$ , where  $\lambda$  is the average wavelength of the X-rays and  $g$  is the gap between mask and sample.  $\sqrt{\lambda g}$  is the linewidth at which the intensity in a narrow line first reaches that of the background with a transparent mask. It assumes single-wavelength coherent illumination. In the limit, a gap of 5  $\mu\text{m}$  might be acceptable for chip lithography and this, with a wavelength of 1 nm, would permit 0.07  $\mu\text{m}$  dimensions to be produced. In the laboratory, intimate contact between mask and resist allows dimensions of a few tens of nanometres to be reached.

(d) *Direct-writing with scanning electron beams*

Electron beams are used for mask-making, in isolated cases for the ‘quick-turn-around’ production of ASICs (application specific integrated circuits), and extensively in research and development but, as already mentioned, they are too slow and expensive for volume manufacturing. Work continues on overcoming this problem because the difficulties facing the practicable implementation of the X-ray alternatives are so severe. Electron beams provide higher resolution than any other method, except local probe atom manipulation, and allow the size of devices to be reduced to the practicable limit of resist processes, which at present falls at about 10 nm.

To increase the throughput of scanning electron-beam systems, methods are being explored in which more and more of the pattern is exposed at each beam flash. It is simplest to write a pattern one pixel at a time with a round electron beam, the diameter of which is equal to the pixel size. This approach is very flexible and accurate but is extremely slow. The next fastest way is to use a beam which can take on any shape up to about four times the minimum feature size (Pfeiffer 1978; Pfeiffer & Groves 1991). This allows tens of pixels to be exposed at each flash and makes it possible to manufacture ASICs. Finally, pattern cells, containing tens of shapes and thousands of pixels, can be projected in a single flash. This is called ‘character’ or

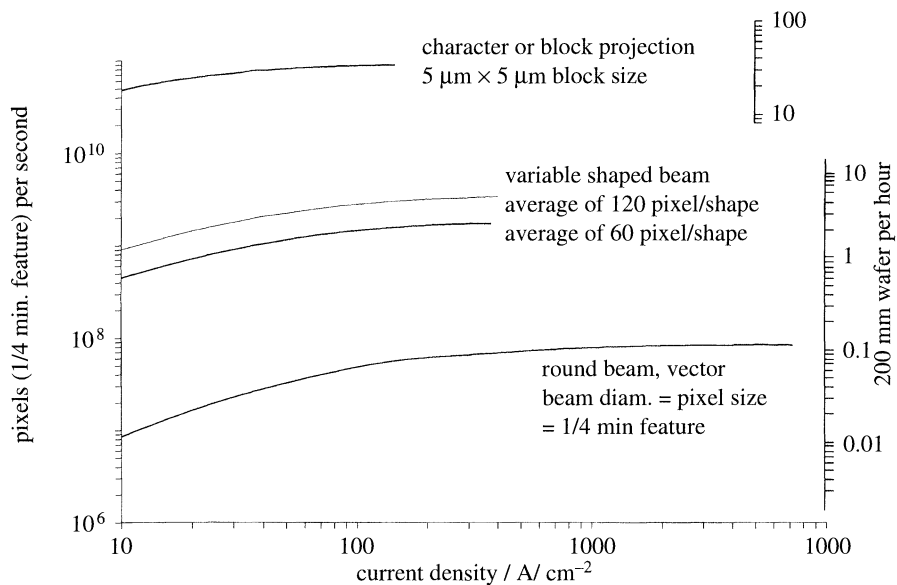


Figure 1. Incrementing rate in pixels per second and wafers per hour as a function of the current density in the beam for the three major types of scanning electron-beam lithography systems.

‘block’ projection and is the only scanning method capable of potentially reaching realistic throughput for pattern replication (Sohda *et al.* 1991; Hattori *et al.* 1993; Sakamoto *et al.* 1993).

Figure 1 shows the throughput as a function of beam current density for examples of the three major types of scanning electron-beam lithography systems. The following parameters were used to calculate the throughput: minimum feature size  $0.2\ \mu\text{m}$ , pixel size  $0.05\ \mu\text{m}$ , pixel delay time for round beam  $10\ \text{ns}$ , shape and character/block delay time  $30\ \text{ns}$ , sub-field delay time  $3\ \mu\text{s}$ , cluster delay time  $200\ \mu\text{s}$ , chip delay time  $100\ \text{ms}$ , wafer change time  $20\ \text{s}$ , fraction of chip areas exposed  $30\%$  for round and shaped beam cases and  $100\%$  for character/block exposure. For higher current densities the throughput and incrementing rate are set by the beam settling times.

In practice, the maximum usable current density is set by electron–electron interactions and therefore upon the total beam current. The electron–electron interactions lead to an increase in velocity spread in the beam which in turn results in beam blurring due to the chromatic aberrations of the focusing lenses and deflection systems. To reduce the interactions, shorter electron-beam columns are used so that electron interaction time is minimized. At present, for round beams, current densities above  $1000\ \text{A cm}^{-2}$  are feasible, but for the shaped and character systems the maximum current density is only about  $100\ \text{A cm}^{-2}$  and  $10\ \text{A cm}^{-2}$ , respectively.

Perhaps the most serious problem facing those who wish to implement character/block projection is that of persuading the chip designers to customize their design rules so that the image can be printed with a finite number of characters or blocks. Customization of design rules to accommodate peculiarities of lithography systems has been considered unacceptable in the past. A further difficulty is that proximity effects, which are discussed later, can only be corrected by changing the shapes of the individual pattern elements because the exposure dose will have to be the same

for all elements in a character or block. Proximity effects are more easily corrected with single beams where it is possible to change the dose as well as the shape.

(e) *Multiple electron beams*

An alternative to exposing many pixels at each beam flash is to use multiple beams. Two distinctly different approaches are being taken to implement this idea. One is a version of the block projection concept in which the character mask is replaced by a multi-aperture mask that in effect produces an array of about 1000 beams (Yasuda 1993). The other is to use ten or more miniature electron-beam columns to write on a single wafer. Each column would have a field emission cathode and would address several chips (Chang *et al.* 1992). There are practical difficulties to be overcome with both approaches. With the large array of beams there is the difficulty of building a multi-deflection unit that can blank and deflect each beam individually and at the same time keep them precisely registered with respect to each other. Control of the beams will be difficult to achieve as the degree of electron–electron interaction in the column will change with the number of beams that are active. The miniature electron optical columns promise very high electron optical performance because of their extremely short focal length, very low aberration, lenses, but severe mechanical tolerances will have to be met to achieve these low aberrations. It will also be difficult to keep the field emission cathodes emitting uniformly and to fabricate the dense array of electron detectors that will be needed to keep track of the individual beams. Overall, there are many problems to be solved before either approach will be a contender for production lithography.

(f) *Electron-beam full pattern projection*

The final possibility for achieving competitive throughput with electron-beam exposure is to build the equivalent of the uv step and repeat camera. The first attempt to do this was in the early 1970s (Heritage 1975). The resolution of the projected image for small field sizes can approach that of an electron microscope, that is a few tenths of a nanometre, and the demagnification can be high enough to make mask fabrication practicable. The first systems demagnified the mask 10 to 20 times. Thin metal stencil masks were used in the early experiments and it was proposed to resolve the difficulties with unsupported and/or fragile features by using two masks for each level. More recently a very thin supporting membrane has been used and the electrons that are scattered by the membrane are removed by the projection lens stopping aperture (Berger & Gibson 1990). Provided the membrane is thin, that is less than  $0.1\ \mu\text{m}$ , and the accelerating voltage is kept relatively high, for example  $> 100\ \text{kV}$ , the loss of current due to scattering can be reduced to about 50%.

The use of a membrane solves some of the mask difficulties, but the scattering reduces the target current density and means that the beam current in the upper column has to be increased, thereby increasing electron–electron interactions. As with the shaped beam scanning systems, the increase in energy spread blurs the image and this effect will ultimately limit the exposure rate. Preliminary estimates suggest that the exposure speed should be adequate, however, at least for dimensions down to  $0.1\ \mu\text{m}$ .

The absorber for the mask can be a relatively thin ( $< 0.1\ \mu\text{m}$ ) layer of a high atomic-weight material, such as gold, that is easy to fabricate. Here the technique has an advantage over X-ray lithography, where the absorber must be up to  $0.4\ \mu\text{m}$  thick, resulting in height to width ratios of 4:1 for dimensions of  $0.1\ \mu\text{m}$ .

A key difficulty with electron-beam projection is pattern distortion. Distortion arises in the mask and in the projection imaging. It should be possible to keep mask distortion at an acceptable level, through the use of supporting ribs which can be fabricated with silicon anisotropic etching, but image distortion will have to be corrected. It is proposed that dynamic corrections be used. The mask will be illuminated with a small beam covering only a fraction of the image and distortion will be corrected by tilting this beam as it is scanned over the mask to complete the exposure. Variable axis condenser and projector lenses will have to be used and the signals to the correction coils in these lenses will have to be extremely accurately synchronized. The size and current in the illuminating beam will be as large as electron–electron interactions allow.

Another major increase in system complexity arises because the lenses become impractically large if the mask plate is to remain stationary and not be scanned. This is the case even if the lenses incorporate variable axis deflectors. Assuming that the lens bores are several, say five, times the size of the mask for the off-axis aberrations to remain correctable, then for a demagnification of 4 and a  $3\text{ cm} \times 3\text{ cm}$  chip, the bore diameter would be  $5 \times 4 \times 3 \times \sqrt{2} = 84\text{ cm}$ . To satisfy the requirement of the magnetic circuit and the excitation coil, the outer diameter of the lens would approach 1.5 m, which would be highly impractical particularly as the column must be kept short to minimize electron–electron interactions. Berger has estimated that the maximum column length will be around 35 cm (Berger *et al.* 1993).

To avoid the large lenses, it is proposed to scan the mask and sample through the optical system, as is done with step-and-scan UV cameras. As a consequence, there will be two scanning mechanisms operating simultaneously. The illumination will be scanned to correct for distortion and the mask and wafer will be scanned to allow the lens diameters to remain practicable. Both condenser and projector lenses will have to be of the moving-axis type because the field sizes will have to be relatively large. The overall complexity will be formidable. It has taken many years to resolve the difficulties with a single variable axis immersion lens in scanning systems where the beam diameter beam is small and there is no mechanical scanning required and no need to scan the illumination. The situation with the projector will be many times more complex.

In summary, electron-beam reduction projection potentially offers higher throughput than character or block projection systems, but the development of a distortion free optical system will be an extremely complex task that will take many years to accomplish.

### (g) Ion beams

Pattern generation and replication systems that use ions have been investigated for many years but there are a number of factors that place them at a disadvantage compared with their electron equivalents. Firstly, they have to use electrostatic lenses which have higher aberrations than the magnetic lenses used with electrons. It is also not possible with electrostatic lenses to overlap focusing and deflection, as can be done with magnetic lenses and coils. Overlapping has been found to be essential with electron-beam systems if adequate field size and beam aperture are to be obtained. Secondly, the effects of particle to particle Coulomb interactions are exaggerated. Thirdly, ion sources have poorer performance in terms of chromatic spread, brightness and/or total current, and, finally, ions do not penetrate resist layers to detect alignment marks, as do electrons.

There is one significant advantage and that is that exposure with ions does not suffer from the deleterious proximity effect encountered with electron exposure because the ions do not penetrate the substrate deeply and hence are not backscattered through the resist into areas away from their intended point of exposure. However, the lack of penetration means that the resist is not exposed uniformly throughout its depth unless high ( $> 100$  kV) accelerating voltages are used. If the energy of the ions is increased until the ions do penetrate through the resist into the substrate then unacceptable damage of the sample may occur. This is not a problem for mask writing, and for direct-writing on semiconductor samples it can be avoided with surface imaging resists, but to date no one has considered the advantage of proximity free exposure to be significant enough to override the shortcomings of ion optical systems.

The ultimate resolution of ion optics is more than 20 times worse than it is for electron optics, *ca.* 5 nm versus *ca.* 0.2 nm (see figure 11), because of the higher aberrations of the electrostatic lenses and the larger energy spread of the sources. This difference is only marginally important for conventional resist exposure, as the resolution of resist itself is about 10 nm, but for inorganic resists, where dimensions well below 10 nm can be obtained, the ion optical resolution limit will become the fabrication limit.

Ion-beam systems have been shown to be valuable for mask and circuit repair, particularly for the removal of unwanted material, but for direct-write lithography they have yet to show any advantage over electron-beam systems either in scanning or projection configurations.

#### (h) Local probes

The difficulty of writing the complex patterns for tomorrow's integrated circuit chips becomes quite clear when one considers what would be required if local probes (as used in atomic force and scanning tunnelling microscopes) were to be used for this task. It has been shown that individual atoms can be manipulated and gold deposited selectively with local probes and it has been suggested that this method might be used for integrated circuit lithography. It would certainly solve all difficulties with respect to resolution, provided of course that suitable processes could be identified, but at the moment the writing rate is far too slow being only a few points per second. Supporters of the concept suggest that it might be possible to write at lateral tip velocities approaching  $1 \text{ cm s}^{-1}$ , which would increase the writing rate to 200 000 pixels  $\text{s}^{-1}$  for 50 nm pixels, and then to use 500 000 tips in parallel to produce the required exposure rate of about 1 second per chip. However, for a wafer diameter of 20 cm, the 500 000 tips and their individual manipulation mechanisms would have to be fabricated on a two-dimensional array with a spacing of approximately 0.1 mm and, to meet cost requirements, each tip together with its manipulator control system associated high-speed data delivery channel would have to cost less than about \$10. Neither of these requirements would seem to be feasible today.

The likelihood that local probes will prove useful in the foreseeable future for chip lithography is therefore small. For scientific work, however, their unique ability to manipulate single atoms makes them ideal for fabricating simple test structures. For example, Eigler and co-workers have created 'quantum corrals' by placed single atoms in a ring with an accuracy of less than 0.1 nm (Crommie *et al.* 1993). This remarkable resolution could not have been obtained by any other method.



### 3. Nanostructure fabrication

#### (a) *Device requirements*

At present, apart from resolution, the requirements for nanostructure devices are considerably less demanding than those for integrated circuits. Most nanometre devices are built for scientific investigation and are relatively simple in form. They are not required in large numbers and the price per device can be orders of magnitude higher than it is for individual components in an integrated circuit. In addition, the yield of good devices need not be high.

Nanostructures are defined to be structures with dimensions below  $0.1\ \mu\text{m}$ . Very high tolerances may have to be met in their fabrication but this is not always necessary. In some cases the devices have to be contacted electrically but methods have been developed for doing this even when the device is made on a fragile membrane. In other cases there may be no need for electrical contact and the device may be assessed using optical methods. Nanostructure devices are very demanding in terms of materials. The materials from which they are made must be extremely uniform and, in many cases, crystallographically perfect. Yet another demanding challenge, and one that has yet to be met, is the development of low-energy etching methods that do not introduce crystallographic defects during patterning.

Because the throughput requirements are relaxed, electron-beam lithography has proved to be ideal for fabricating nanostructures and has been used in almost all instances. The frustrating aspect of electron-beam lithography is that there are no fabrication processes capable of reproducing the minimum image features that can be resolved by the optical systems. This is discussed in the next subsection.

#### (b) *Electron-beam lithography—resolution limits*

The ultimate resolution of electron-beam lithography is set by the fabrication process and not by the resolution of electron optical systems, which can approach  $0.1\ \text{nm}$ . Electron-beam lithography is unique amongst the non-local probe methods in this characteristic. Provided the highest resolution resists are used, the resolution of all other methods, with the exception of STM manipulation, is limited by the resolution of the imaging systems. Of course, when high throughput is important, the resolution with electron-beam systems may also become limited by the electron optics.

There is a long history of structure fabrication with electron microscopes and related instruments.  $50\ \text{nm}$  features were written into a collodion film (Mollenstedt & Speidel 1960), the first potentially useful structures,  $50\ \text{nm}$  metal wires, were produced in 1964 (Broers 1964, 1965), and the first functional devices with linewidths beyond the capability of optics, which were surface acoustic wave devices with  $0.15\ \mu\text{m}$  fingers, were fabricated and tested in 1969 (Broers *et al.* 1969), see figure 2.

It was clear from the beginning that the resolution of the electron optical system was not the limiting factor. The diameter of the electron beam in the early experiments was many times smaller than the structures that were fabricated. For example, the  $50\ \text{nm}$  metal linewidths fabricated in 1964 were written with a beam that was about  $10\ \text{nm}$  in diameter. The limit was thought to be set by electron scattering in the resist and perhaps by the resist itself. The contribution by electron scattering was clarified by Chang (1975) who pointed out that the two major types of scattering could be treated separately and modelled by Gaussian distributions. The first of these, called forward scattering, is the small angle inelastic scattering of the electrons

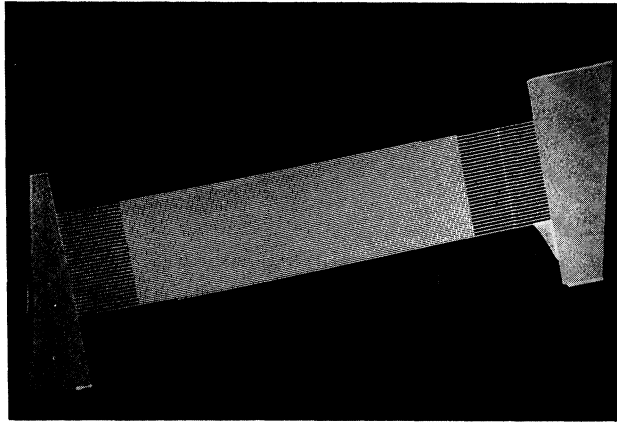


Figure 2. 3.5 GHz surface acoustic-wave delay line fabricated in 1969 with electron-beam lithography. The centre to centre spacing of the aluminium fingers is  $0.5\ \mu\text{m}$ .

as they penetrate the resist. It is modelled by the narrower of the distributions. With thin resists ( $< 0.1\ \mu\text{m}$ ) and high accelerating voltages ( $> 100\ \text{kV}$ ) its width becomes negligible (*ca.*  $1\ \text{nm}$ ). The second, which is called backscattering, is the large angle elastic scattering that occurs mainly in the substrate beneath the resist. Electrons are backscattered from the substrate into and through the resist. The total exposure due to backscattered electrons is roughly equal to the exposure produced by the incoming electrons, but it is spread out over a diameter that is roughly equal to the range of the electrons in the substrate. For high accelerating voltages, this is very large compared to the width of the forward scattering distribution. For example, it is about  $30\ \mu\text{m}$  for  $100\ \text{kV}$  electrons and a silicon substrate. The backscattered electrons, in effect, produce a background fog that reduces contrast. It does not directly limit the ultimate resolution. It turns out that the ultimate resolution is determined by other factors, as discussed in the next subsection.

Implementation of electron-beam lithography was hampered through the 1970s because most systems were operated at about  $20\ \text{kV}$ , where the width of the backscattered distribution is  $2\text{--}3\ \mu\text{m}$ , which is close to the  $1\ \mu\text{m}$  linewidths that were being fabricated. In this regime, exposure at any point in the pattern is strongly affected by exposure of adjacent features. As a consequence, this effect, which was called the ‘proximity effect’ by Chang (1975), received a vast amount of attention and elaborate computational methods were developed for adjusting the exposure dose from shape to shape to minimize its effect. Recently it has been realized that these are not necessary if exposure is made at higher voltages, where the backscattered distribution is large compared to the pattern features and relatively simple compensation algorithms are satisfactory. It is also possible to reduce proximity effect by operating at low voltages and using resists in which only a thin surface layer is active. The thin active layer reduces the width of the forward scattering distribution and the energy of the electrons can be reduced to the point that the width of the backscattered distribution is also small. To reduce the backscattered width to less than  $0.1\ \mu\text{m}$ , however, requires electron energies below  $1\ \text{kV}$ , where the performance and stability of the electron optical system deteriorates rapidly.

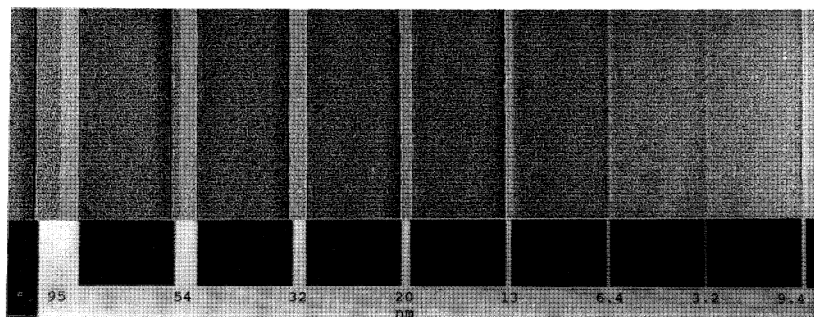


Figure 3. Transmission electron micrograph of part of the test pattern used to evaluate the point spread function for PMMA. The lower half of the figure is the directly recorded image without a sample, that is the written pattern, and the upper half is the image of a developed and shadowed PMMA pattern.

(c) *Ultimate resolution of conventional resist (PMMA)*

The ultimate resolution of resist exposure with electrons is not set by electron scattering, as this can be made to be negligible by using thin resist and high accelerating potential, but by a combination of: (i) the delocalization of the exposure process, as determined by the range of the Coulomb interaction between the electrons and the resist molecules (Lutwyche 1992); (ii) the straggling of secondary electrons into the resist; (iii) the molecular structure of the resist; and (iv) the molecular dynamics of the development process. The relative contribution of the four factors is not known but their overall effect can be modelled by the ‘point spread’ function for the resist. This function has been accurately measured for PMMA, the highest resolution resist known. Figure 3 shows the type of pattern used to determine the point spread function for PMMA and figure 4 illustrates the exposure mechanisms limiting resolution.

Using the resist point spread function, together with the forward scattering and backscattering distributions, it is possible to calculate the exposure distribution for thin and thick substrates and hence the resolution and contrast for electron lithography for most real situations (Broers 1980, 1981). The measurement of the point spread function was originally made with a 0.5 nm diameter electron beam, a resist thickness of 60 nm and an accelerating voltage of 50 kV for which conditions electron scattering and the beam diameter were negligible. The measurement was later repeated for 350 kV exposure (Broers *et al.* 1989) and again more recently using improved methods for determining the point at which the lines in the test pattern develop out (Hoole 1993). The results are the same within the experimental error of the measurements. The point spread function is measured by determining the relative dose required for complete development of lines that have precisely ‘written’ widths that are narrower than the function’s width. The method is designed to completely avoid the measurement of actual resist linewidths, because this is virtually impossible due to electron damage during observation.

It is not easy to establish a criterion for the minimum size for isolated features because this varies with resist exposure and development conditions. Resist patterns also become rapidly distorted under electron irradiation, making them difficult to examine in an electron microscope. It is generally better to ‘lift off’ a thin metal pattern and examine this in an electron microscope. Provided the metal film is smooth and featureless it will accurately replicate the resist pattern. An SEM must be used

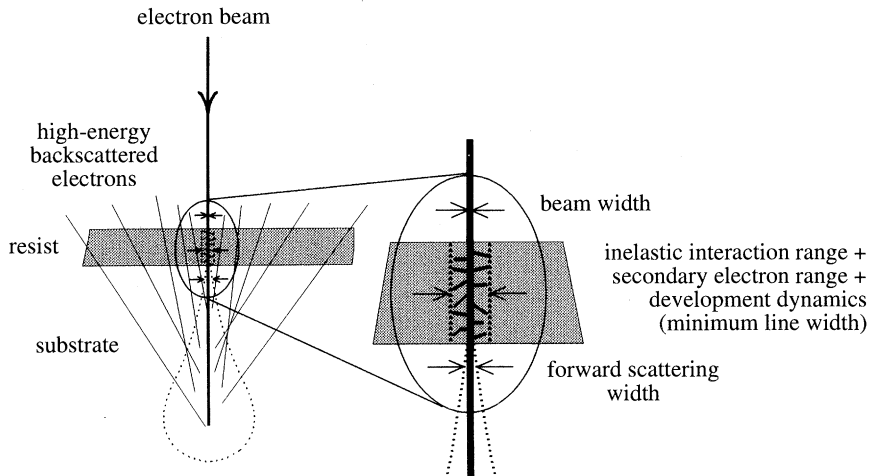


Figure 4. Mechanisms contributing to exposure of resist with an electron beam. The ultimate resolution is set by the exposure and development process and not by electron scattering or by the electron optics. A 'point-spread function' for the process can be determined experimentally and used together with the widths of the forward and backscattering distributions to show that the minimum centre-to-centre spacings for an infinitely large array of equal lines and spaces is about 20 nm for a thin substrate and 25 nm for a bulk (silicon) substrate (Broers 1980, 1981).

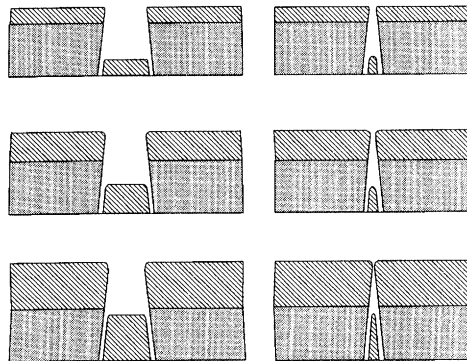


Figure 5. Resolution limit for lift-off patterning. The width of the lifted-off line is determined by the width of the resist line at the surface, the minimum centre-to-centre spacing is set by the undercut and the thickness of the resist, and the maximum thickness of material depends on the thickness of the resist. A falsely optimistic estimate of linewidth will be obtained if the sample is examined before the metal is lifted off.

if the pattern is on a bulk substrate but it is better from a resolution point of view to use a thin substrate and a transmission electron microscope. The metal has to be extremely thin ( $< 3$  nm) if accurate data are to be obtained. A falsely optimistic result will be obtained if the sample is examined before the metal is lifted off because the metal overhangs the edges of the lines making the gap in the metal narrower than that in the resist. This is illustrated in figure 5. Figure 6 shows a lifted-off pattern with the smallest dimensions that can be obtained with PMMA.

Studies of the edge roughness of resist lines have revealed that in two component resists the backbone resin of the resist is important. An example is cited in which a polyvinylphenol-based resist exhibits finer edge roughness than a novolak based

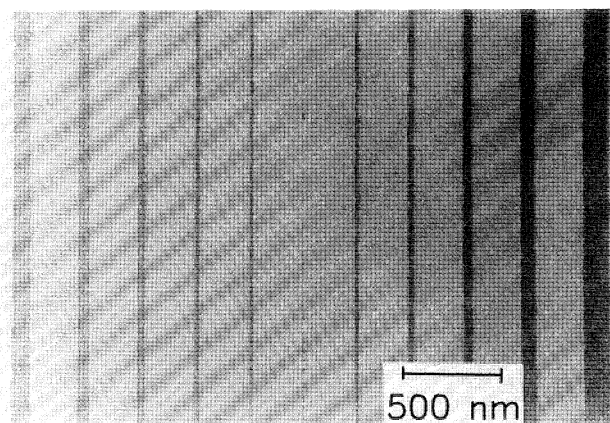


Figure 6. Au–Pd pattern demonstrating the resolution limit of lift-off with PMMA. The narrowest line, with a nominal width of 3.2 nm has not lifted off. The second narrowest line, with a nominal width of 6.4 nm is discontinuous. The 9.4 nm line is continuous to the extent that the metal film is continuous.

resist (Yoshimura 1993). A molecular model has also been developed which allows the structure of the resist to be followed through exposure and development (Scheckler *et al.* 1993). When operating with the highest resolution resist such as PMMA, it has been suggested that residual edge roughness may be the result of small fluctuations in beam current.

#### (d) *Vapour resist*

A number of nanometre size devices have been made using, as a resist, the carbonaceous deposit (commonly called contamination) that builds up at the point of impact of an electron beam when hydrocarbon molecules are present on the surface. The hydrocarbons may be present on the surface due to: (i) previous immersion of the sample in a vacuum system with a high partial pressure of hydrocarbons; (ii) arrival from the residual vacuum of the electron-beam lithography system; or (iii) delivery to the point of impact of the beam via a capillary needle. In the first two cases the writing rate may decline as writing continues due to depletion of the hydrocarbons. With the direct delivery of vapour via a capillary, it is possible to maintain a constant writing rate. In all cases the exposure dose required is several orders of magnitude higher than for the conventional resists, being  $0.1\text{--}1\text{ C cm}^{-2}$ .

The point spread function for vapour resist has not been measured but it is apparent that the ultimate resolution is similar to that of conventional resist. For example, when it is used as a mask for dry etching of metal structures, linewidths down to a minimum of about 5 nm are obtained. For linewidth control of 10% or better, the minimum is closer to 15 nm. Again it is unclear whether the limit is due to the range of interaction of the electrons with the resist or due to the mechanism with which the hydrocarbons are cracked into a stable compound on the surface. Figure 7 shows a high resolution nanostructure fabricated with contamination resist and ion milling (Broers *et al.* 1989).

#### (e) *Direct sublimation (hole drilling) with electron beams*

Certain materials can be directly sublimated with an electron beam with extremely high resolution. This process was discovered with the ‘drilling’ of 5 nm diameter holes

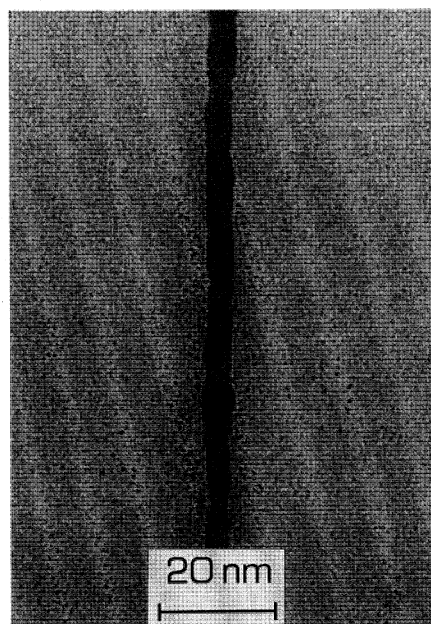


Figure 7. Au-Pd line with an average width of *ca.* 5 nm formed with vapour resist and ion milling.

through a  $0.25\ \mu\text{m}$  NaCl crystal (Broers *et al.* 1978). Subsequently, a variety of other materials have been shown to behave in a similar manner and, for example, holes as small as 1 nm have been drilled in  $\text{Al}_2\text{O}_3$  (Mochel *et al.* 1983). The resolution of the process is perhaps higher than that of any other electron-beam process, presumably because it requires a relatively large quantum of energy to activate and is therefore more closely localized to the electron beam. However, there are difficulties in fabricating useful devices. First of all the holes are not 'clean'. Clean holes are formed through membranes where the material can be sublimated from both sides of the membrane, but on a bulk substrate a deposit remains in the exposed areas. The deposit is rich in one of the elements of the drilled compound. For metallic compounds it has been shown with electron energy-loss spectroscopy that a metal rich deposit remains and it has been suggested that metal wires might be formed in this way for device applications. The insensitivity of the process and the lack of purity of the metal limit the usefulness of this method. The deposit also prevents the drilled patterns being used satisfactorily as masks for wet etching. Dry etching cannot be used either because the materials that can be drilled have poor resistance to dry etching. Other disadvantages are the extreme insensitivity (*ca.*  $100\ \text{C cm}^{-2}$  at room temperature, *ca.*  $10\ \text{C cm}^{-2}$  at *ca.*  $200\ ^\circ\text{C}$ ) of the process and its highly non-linear dose/exposure relationship, which means that no patterns are formed until a very high exposure threshold is reached. The latter leaves little flexibility in the exposure conditions. Reciprocity is only attained at current densities of more than  $1000\ \text{A cm}^{-2}$ .

It may be possible to use the method to provide templates for selective deposition of thin films, either through low-angle evaporation or through any other selective deposition process, but this has yet to be done. The use of templates is discussed later.

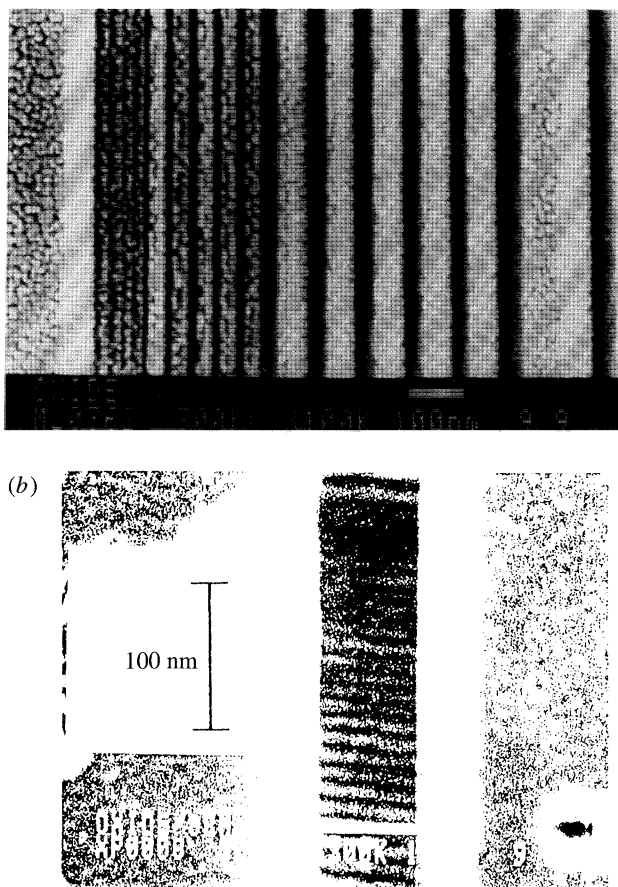


Figure 8. (a) Structures etched with HF-acid-based etches in  $\text{SiO}_2$  layers after e-beam irradiation. (b) High resolution test pattern in  $\text{SiO}_2$ ; 250 nm thick  $\text{SiO}_2$  layer is supported on 150 nm  $\text{Si}_3\text{N}_4$  membrane.

(f) *Electron-beam exposure of  $\text{SiO}_2$  layers: charge patterns and structures*

In 1968 it was discovered that the etch rate of  $\text{SiO}_2$  could be enhanced by electron bombardment and that this process could be used to fabricate structures (O'Keefe & Handy 1968). Electron exposure at a high dose rate of  $1\text{--}5\text{ C cm}^{-2}$  produces a three times increase in the etch rate of the  $\text{SiO}_2$  in hydrofluoric-acid-based etches. A re-examination of the process by Allee *et al.* (1990) revealed that it had extremely high resolution (see figure 8a). Arrays of lines and spaces with a centre-to-centre spacing of 20 nm were produced. Subsequently, an 11 nm period has been achieved by Pan & Broers (1993), as shown in figure 8b. These results show that the width of the point spread function for the process is less than half that of PMMA. A key to the successful implementation of the  $\text{SiO}_2$  process is the prevention, or removal, of the layer of contamination that forms on the surface during writing. A number of methods have been used to avoid this problem, the simplest being to heat the sample to about  $150^\circ\text{C}$  during writing to prevent the contamination forming in the first place.

The process works well with high-quality grown oxide of the type used as the gate oxide in field effect transistors and it is possible, in principle, to pattern a gate oxide

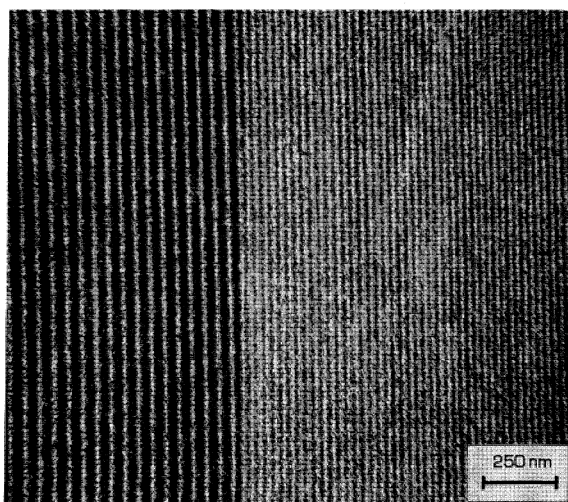


Figure 9. Lines written in a stack of Langmuir–Blodgett films using a 1 nm diameter, 50 kV electron beam (Broers *et al.* 1978).

to produce short gate length or superlattice devices. A metal or semiconductor gate would be placed on top of the oxide and the channel modulated according to the thickness of the  $\text{SiO}_2$ .

An oxide layer, patterned by the direct-exposure process can also be used as a mask for dry etching of single crystal and polycrystalline silicon. 10 nm wide cuts have been made in this way and the process used to pattern polycrystalline silicon gates.

The mechanism of the direct-exposure process is not understood but it is likely that it is connected with the creation of ionized species within the oxide, effectively the storage of charge. It was observed by Pan (personal communication) that the charge pattern written by the beam can be seen in a secondary electron scanning electron micrograph and micrographs taken from different angles imply that the beam induces conductivity through the oxide. This suggests that it may be possible to make devices by merely writing charge patterns into the oxide without actually producing an etched structure. The charge distribution could, in principle, be used to modulate the channel in a field-effect device. Alternatively, the charge pattern could be decorated by a variety of methods similar to electroplating. A Xerographic-like process might be envisaged in which polar molecules would be selectively deposited to produce a structure with molecular dimensions.

#### (g) Langmuir–Blodgett films

Several authors have used the Langmuir–Blodgett (LB) method to coat samples with electron-beam sensitive films (Kuan *et al.* 1989). Conventional resist layers with thicknesses approaching the size of single molecules have been deposited. Unfortunately, the lateral resolution of electron-beam exposure is not set by the thickness of the resist and so this has not yielded any improvement in resolution.

It is also possible to write directly in LB films and produce high-resolution periodic patterns. For example, figure 9 shows lines on 25 nm centres written at  $10^{-8} \text{ C cm}^{-1}$  in 138 layers of manganese stearate (Broers & Pomerantz 1983). Block areas of this



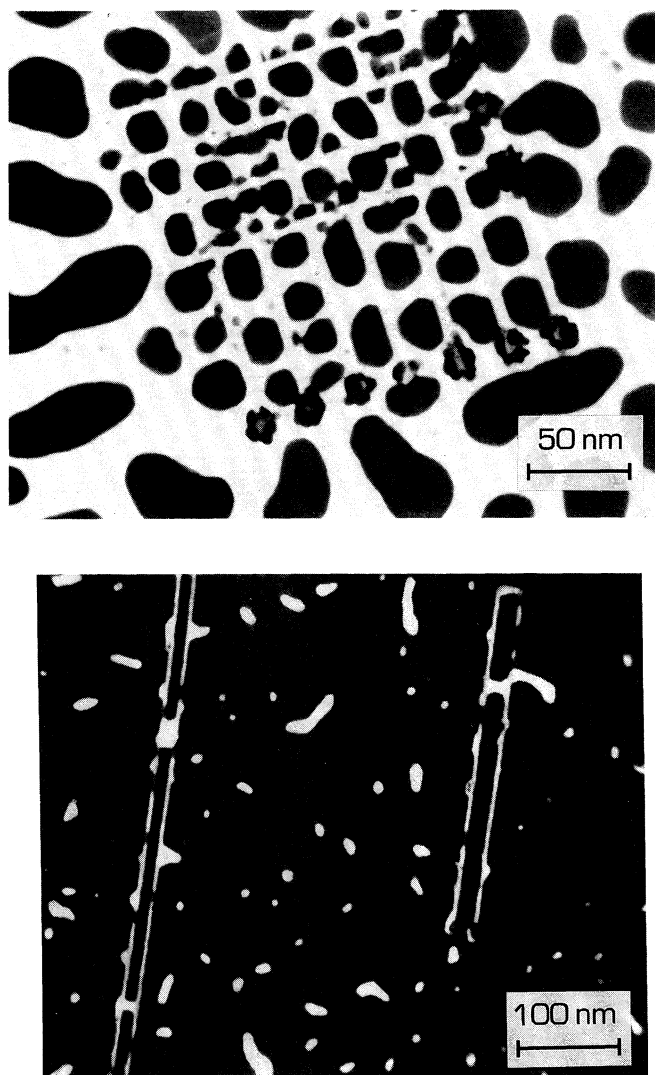


Figure 10. Patterns created by evaporating lead on top of vapour resist templates.

sample became exposed with  $10^{-3} \text{ C cm}^{-2}$ . The centre-to-centre spacing is equal to the best that can be obtained with PMMA. Finer lines might also have been observed but it is difficult to obtain satisfactory micrographs of them because the electron irradiation required to obtain the images also exposes the films. The writing mechanism is complex. The beam initially induces mass loss, presumably by sublimation, because the lines appear bright when viewed with bright field transmission electron microscopy. However, if, after the lines are written, the general areas surrounding the lines are exposed with a large average dose, the originally bright lines appear dark against a light background, as shown in figure 16 of Broers *et al.* (1978). To the author's knowledge, patterned LB films of materials other than PMMA have not been used successfully as masks for wet or dry etching. As with the direct sublimation

processes, the most likely route for practicable application is to use the patterned films as templates.

(h) *Templates for thin-film deposition*

It is possible to influence the deposition of thin films by creating artificial topography on a surface. This has been accomplished in a number of ways: for example, with regular steps it is possible to influence the orientation of a single crystal film in a process that has been called 'graphoepitaxy' by Geis *et al.* (1979). The author has attempted the fabrication of non-regular structures through the use of electron-beam vapour resist structures on a silicon surface. The vapour resist lines were written with a 50 kV electron beam at a dose that produced lines approximately 0.1  $\mu\text{m}$  thick and 10–20 nm wide. A lead film 50 nm thick was then evaporated onto the sample. Figure 10 shows that the lead did not deposit on the crests of the lines, thereby producing gaps, but did deposit in the troughs between the lines forming what might have become continuous lines. It is unlikely that useful structures can be produced in this manner unless the method is combined with single-atom manipulation, but it illustrates the concept of template patterning.

(i) *Direct formation of Josephson junctions*

Selective irradiation of high-temperature superconductors with high-energy electrons has been shown to produce high-quality Josephson junctions (Pauza *et al.* 1993, 1994). The process is believed to involve the selective removal of oxygen from the films. The junctions, which are produced by irradiation at an electron energy of 350 kV and a dose of about 1000  $\text{C cm}^{-2}$ , exhibit extremely uniform characteristics and show a high quality Fraunhofer structure in the variation of the critical current with magnetic field. The beam current during writing is typically 2 nA and the beam is used to write the junction across a track with a width about 3  $\mu\text{m}$ . The width of the junctions is thought to be 10–20 nm, although the diameter of the beam was less than 5 nm.

#### 4. Conclusions

As the dimensions of integrated circuit are reduced below 0.1  $\mu\text{m}$ , new production methods will be needed for pattern replication. A wide variety of methods are being explored to meet this need, but the task is daunting and most of the new methods will fail to produce the high-complexity distortion-free images at acceptable cost. Some of the leading contenders have been discussed in this paper, including soft X-ray projection, X-ray lithography and scanning electron-beam lithography. The data needed to decide which of the new methods will be most successful are not available and it is certainly not possible to predict the sequence in which they will be implemented.

The resolution limits of the different methods can be estimated more easily and these have been discussed in some detail in this paper. Ultimately, the highest resolution method for producing artificial structures is to fabricate them atom by atom with a local probe. This is impractically slow, however, even for nanostructure devices, and in addition, no means have been found to make electrical contact to structures of this scale, although there is no reason why eventually this should not be done. Most useful electronic devices have been made with conventional electron-beam lithography, but even these have been relatively simple and the writing rate only adequate to make a few devices.

Table 1. *Practical and ultimate resolution limits for lithography methods*

lithography type	practical limit	ultimate limit
ultraviolet light contact/proximity	2.5 $\mu\text{m}$ Fresnel diffraction at minimum practicable gap and wavelength. Wavelength 200 nm, gap 25 $\mu\text{m}$	0.125 $\mu\text{m}$ Fresnel diffraction for contact print with 100 nm thick resist. Wavelength 160 nm, gap 100 nm
X-ray proximity	0.07 $\mu\text{m}$ Absorber aspect ratio and Fresnel diffraction at practicable gap for step and repeat operation. Wavelength 10 nm, gap 5 $\mu\text{m}$	0.01 $\mu\text{m}$ Fresnel diffraction for contact print and resist resolution limit. Wavelength 1 nm, gap 100 nm
ultraviolet light projection	0.15 $\mu\text{m}$ Fraunhofer diffraction at NA set by fabrication and field-size limits with phase shift mask, etc. Wavelength 157 nm, NA 0.75, depth of focus 0.3 $\mu\text{m}$	0.01 $\mu\text{m}$ Fraunhofer diffraction at wavelength set by transparency of resist and optical materials. Wavelength 157 nm, NA 0.9, depth of focus 0.2 $\mu\text{m}$ , field size < 200 $\mu\text{m}$
soft X-ray projection	0.05 $\mu\text{m}$ Fraunhofer diffraction at NA set by achievable tolerances on optical components. Wavelength 13–13 nm, NA 0.1, depth of focus 1.4 $\mu\text{m}$	0.01 $\mu\text{m}$ Fraunhofer diffraction and resist resolution limit. Wavelength 2–5 nm, NA 0.2, depth of focus 0.07 $\mu\text{m}$ , field size ??
electron beam	0.03–0.05 $\mu\text{m}^{\text{a}}$ lateral scattering of electrons in resist and/or interaction range of exposure process. Accelerating voltage 100 kV	0.007–0.02 $\mu\text{m}$ (resist) delocalization of exposure (secondary electrons)  0.001–0.005 $\mu\text{m}$ (direct exposure/sublimation) combination of electron interaction range and electron optical limits (diffraction and spherical aberration)
ion beam	0.03–0.05 $\mu\text{m}^{\text{a}}$ ion optical limits (chromatic aberration) and interaction range with resist	0.01–0.02 $\mu\text{m}$ (resist) delocalization of exposure (secondary electrons) and ion optical limits (chromatic aberration)  0.01 $\mu\text{m}$ (ion milling) delocalization of sputtering process

<sup>a</sup>In practice, resolution is more often limited by the beam size or aperture as determined by throughput needs.

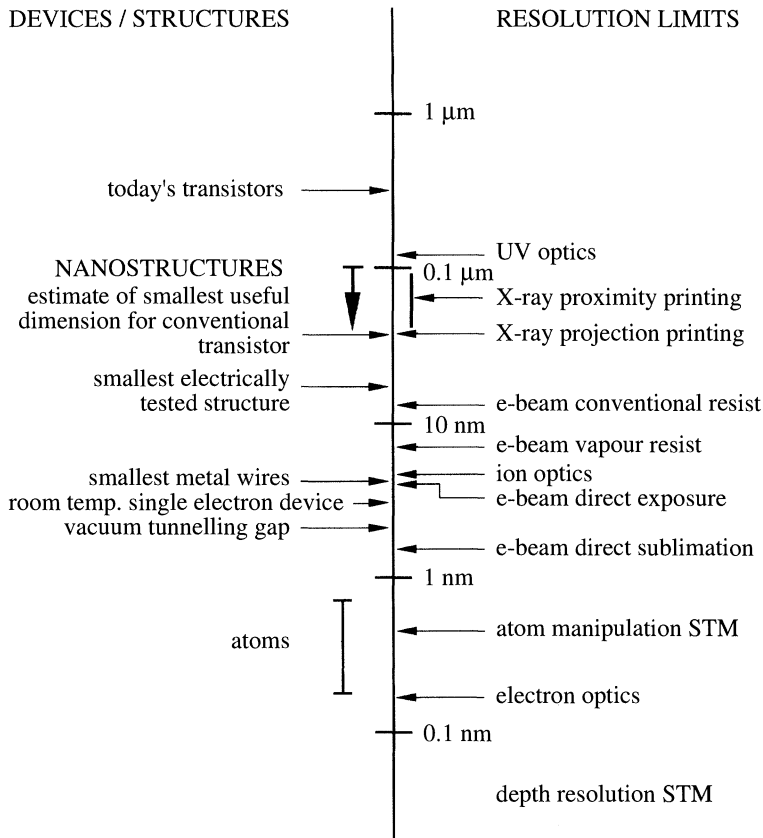


Figure 11. Scale giving the sizes of various devices and structures and the resolution of optical systems and lithography methods.

The size scale in figure 11 shows the dimensions of nanometre-size devices and structures together with the capabilities and resolution of the various imaging and fabrication methods. A range is given for the resolution of X-ray lithography that reflects the extremes of a practicably gap for manufacturing (5–10  $\mu\text{m}$ ) and in-contact printing in the laboratory where mask and wafer touch each other and the gap is set by the resist thickness ( $< 1 \mu\text{m}$ ).

Table 1 summarizes the resolution limits of the different lithography methods. The ‘practical limit’ in this table is the limit that should be achieved in production, and the ‘ultimate limit’ is that which may be achieved in the laboratory under ideal conditions. Table 2 compares the different electron-beam nanofabrication and nanostructuring methods.

The work discussed in this paper has been described by many workers in publications that are too numerous to cite comprehensively. Further reading is available in the Proceedings of the International Symposia on Electron Ion and Photon Beams, published each year in the Journal of Vacuum Science and Technology; the Proceedings of the International Conferences on MicroProcess, published each year in the Japanese Journal of Applied Physics; and the Proceedings of the Microcircuit conferences, published by Elsevier.

Table 2. Resolution, sensitivity and application of high resolution electron beam nanolithography methods

process	resist		structures		sensitivity	useful devices
	smallest isolated features	minimum cntr/cntr spacing	smallest isolated features	minimum cntr/cntr spacing		
spin-on resist (PMMA +ve)	7–10 nm	30–50 nm	10 nm	40–50 nm	$10^{-4}$ C cm <sup>-2</sup>	yes
vapour resist (contamination)	5–8 nm	40–50 nm	5–8 nm	40–50 nm	$10^{-1}$ C cm <sup>-2</sup>	yes
direct sublimation (NaCl, AlF <sub>3</sub> ...)	0.5–2.0 nm	4 nm	10 nm	20–30 nm	10 C cm <sup>-2</sup>	no
direct exposure (SiO <sub>2</sub> )	?3–10 nm	?15 nm	5–10 nm	15 nm	2–5 C cm <sup>-2</sup>	no
direct-exposure high $T_c$ superconductors	?30 nm	?	?30 nm	?	> 200 C cm <sup>-2</sup>	yes

The author acknowledges his colleagues, Dr Xiaodan Pan and Dr Andrew Hoole, with whom he has been working in Cambridge on the limits of resolution for electron-beam lithography.

### References

- Allee, D. R. & Broers, A. N. 1990 *Appl. Phys. Lett.* **57**, 2271.
- Berger, S. D. & Gibson, J. M. 1990 *Appl. Phys. Lett.* **57**, 153.
- Berger, S. D., Eaglesham, D. J., Farrow, R. C., Freeman, R. R., Kraus, J. S. & Liddle, J. A. 1993 *J. Vac. Sci. Technol. B* **11**, 2294–2298.
- Broers, A. N. 1964 *Proc. 1st Int. Conf. on Electron and Ion Beam Science and Technology* (ed. R. Bakish), pp. 191–204. New York: Wiley.
- Broers, A. N. 1965 *Microelectronics and reliability* vol. 4, pp. 104–104. London: Pergamon.
- Broers, A. N. 1981 *IEEE Trans. Electron Devices* ED-**28**, 1268–1278.
- Broers, A. N. 1980 *J. electrochem. Soc.* **128**, 166–170.
- Broers, A. N. & Pomerantz, M. 1983 *Thin Solid Films* **99**, 323–329.
- Broers, A. N., Lean, E. G. & Hatzakis, M. 1969 *Appl. Phys. Lett.* **15**, pp. 98–110.
- Broers, A. N., Cuomo, J. J., Harper, J., Molzen, W., Laibowitz, R. B. & Pomerantz, M. 1978 *Electron microscopy* (ed. J. M. Sturgess), vol. III, pp. 343–354. Toronto: Microscopical Society of Canada.
- Broers, A. N., Timbs, A. E. & Koch, R. 1989 *Microelectronic Engng* **89**, 187–190.
- Chang, T. H. P. 1975 *J. Vac. Sci. Technol.* **12**, 1271–1275.
- Chang, T. H. P., Kern, D. P. & Muray, L. P. 1992 *J. Vac. Sci. Technol. B* **10**, 2743–2748.
- Coopmans, F. & Roland, B. 1987 *Solid St. Technol.* **30**, no. 6, 93–99.
- Crommie, M. F., Lutz, C. P. & Eigler, D. M. 1993 *Nature* **363**, 524–527.

- de Beeck, M. O. & Van den Hove, L. 1992 *J. Vac. Sci. Technol. B* **10**, 701–714.
- Geis, M. W., Flanders, D. C. & Smith, H. I. 1979 *J. Vac. Sci. Technol.* **16**, 1640–1643.
- Hattori, K. *et al.* 1993 *J. Vac. Sci. Technol. B* **11**, 2346–2351.
- Heritage, M. B. 1975 *J. Vac. Sci. Technol.* **12**, 1135.
- Kuan, S. W. J., Frank, C. W., Lee, Y. H. Y., Eimon, T., Allee, D. R., Pease, R. F. W. & Browning, R. 1989 *J. Vac. Sci. Technol. B* **7**, 1745–1750.
- Kurihara, K., Kinoshita, H., Mizota, T., Haga, T. & Torii, Y. 1991 *J. Vac. Sci. Technol. B* **9**, 3189–3192.
- Lutwyche, M. I. 1992 *Microelectronic Engng* **17**, 17–20.
- Mochel, M. E., Humphreys, C. J. & Mochel, J. M. 1983 *Proc. 41st Annual Meeting of the Electron Microscopy Society of America*, pp. 100–101. San Francisco, CA: San Francisco Press.
- Mollenstedt, G. & Speidel, R. 1960 *Phys. Blatter* **16**, 192.
- Okazaki, S. 1991 *J. Vac. Sci. Technol. B* **9**, 2829–2833.
- O'Keefe, T. W. & Handy, R. M. 1968 *Solid state electronics*, vol. 11, pp. 261–266. London: Pergamon.
- Pan, X. D & Broers, A. N. 1993 *Appl. Phys. Lett.* **63**, 1441–1442.
- Pauza, A. J., Campbell, A. M., Moore, D. F., Somekh, R. E. & Broers, A. N. 1994 *Physica B* **194–B196**, 119–120.
- Pauza, A. J., Campbell, A. M., Somekh, R. E. & Broers, A. N. 1993 *IEEE Trans. Appl. Supercond.* **AS-3**, 2405.
- Pfeiffer, H. C. 1978 *J. Vac. Sci. Technol.* **15**, 887.
- Pfeiffer, H. C. & Groves, T. R. 1991 *Microelectronic Engng* **13**, 141.
- Sakamoto, K. *et al.* 1993 *J. Vac. Sci. Technol. B* **11**, 2357–2361.
- Scheckler, E. W., Shukuri, S. & Takeda, E. 1993 *Jap. J. Phys.* **32**, 327–333.
- Sedgwick, T. O., Broers, A. N. & Agule, B. J. 1972 *J. electrochem. Soc.* **119**, 1769–1771.
- Smith, H. I. & Schattenburg, M. L. 1992 *Proc. SPIE Symp. on Microlithography (San Jose, CA)*.
- Sohda, Y. *et al.* 1991 *J. Vac. Sci. Technol. B* **9**, 2940–2943.
- Spears, D. L. & Smith, H. I. 1972 *Electronics Lett.* **8**, 102–104.
- Tennant, D. M. *et al.* 1991 *J. Vac. Sci. Technol. B* **9**, 3176–3183.
- White, D. L. *et al.* 1991 *Solid St. Technol.* **34**, no. 7, 37–42.
- Yasuda, H. 1993 *Proc. Microprocess Conf.*
- Yoshimura, T., Shiraishi, H., Yamamoto, J. & Okazaki, S. 1993 *Appl. Phys. Lett.* **63**, 764–766.

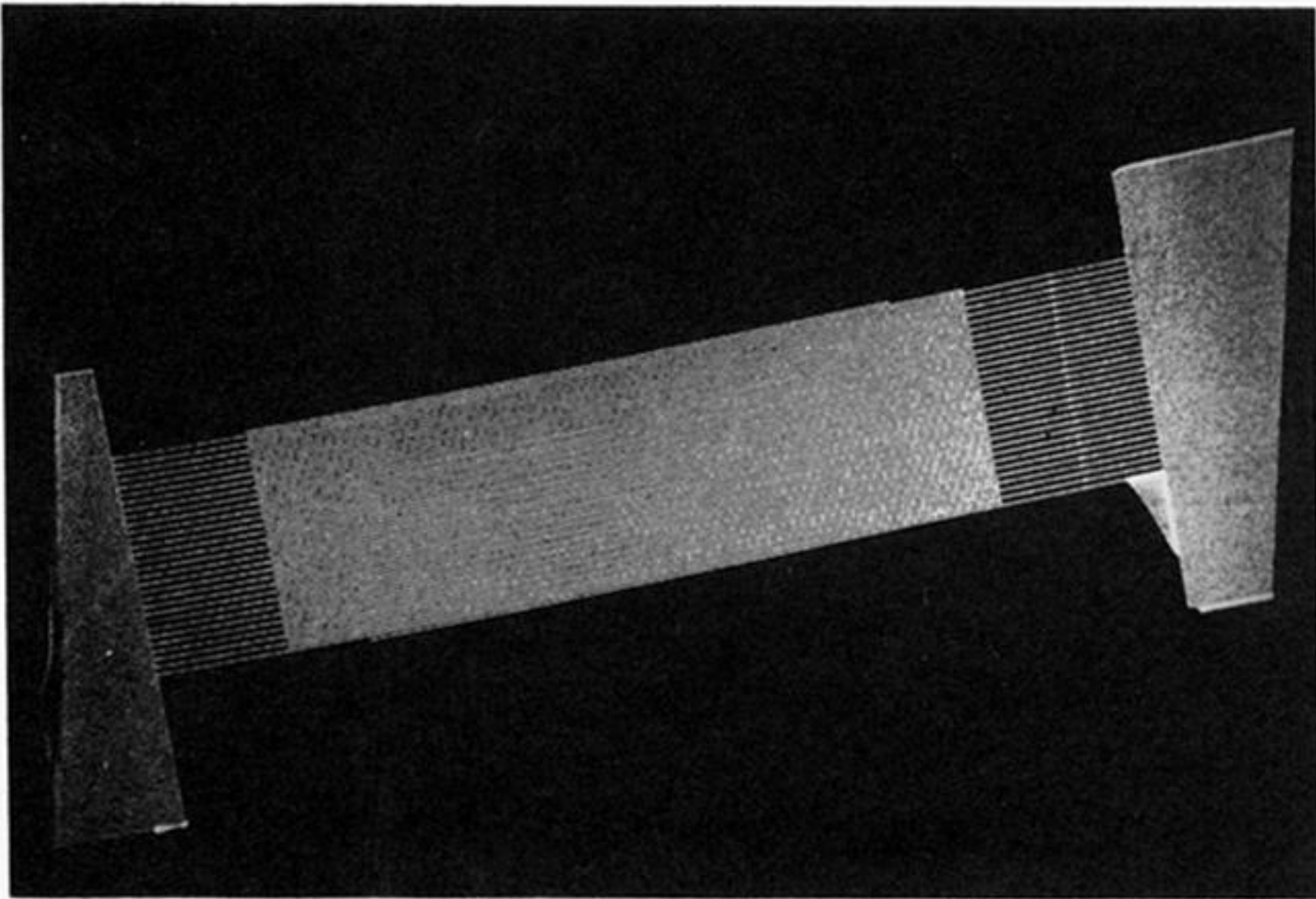


Figure 2. 3.5 GHz surface acoustic-wave delay line fabricated in 1969 with electron-beam lithography. The centre to centre spacing of the aluminium fingers is  $0.5 \mu\text{m}$ .

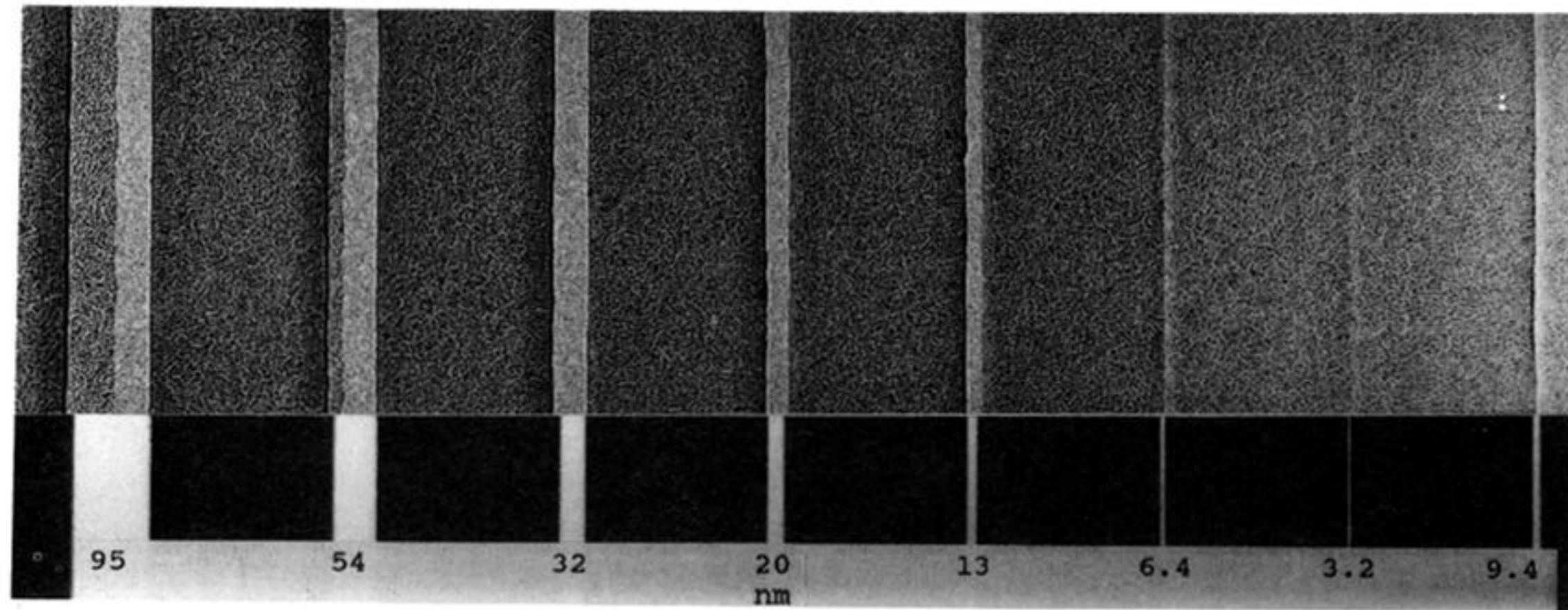


Figure 3. Transmission electron micrograph of part of the test pattern used to evaluate the point spread function for PMMA. The lower half of the figure is the directly recorded image without a sample, that is the written pattern, and the upper half is the image of a developed and shadowed PMMA pattern.



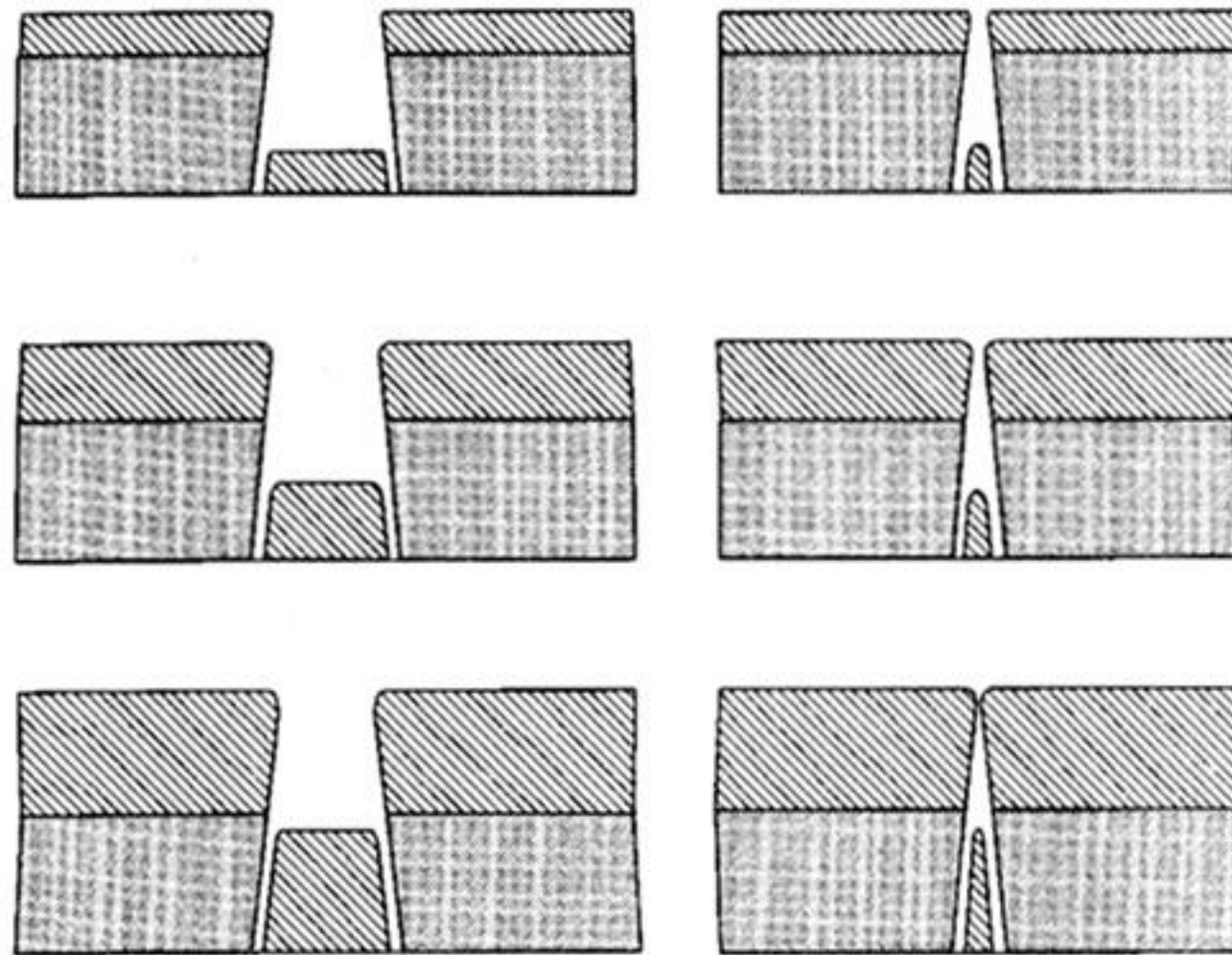


Figure 5. Resolution limit for lift-off patterning. The width of the lifted-off line is determined by the width of the resist line at the surface, the minimum centre-to-centre spacing is set by the undercut and the thickness of the resist, and the maximum thickness of material depends on the thickness of the resist. A falsely optimistic estimate of linewidth will be obtained if the sample is examined before the metal is lifted off.

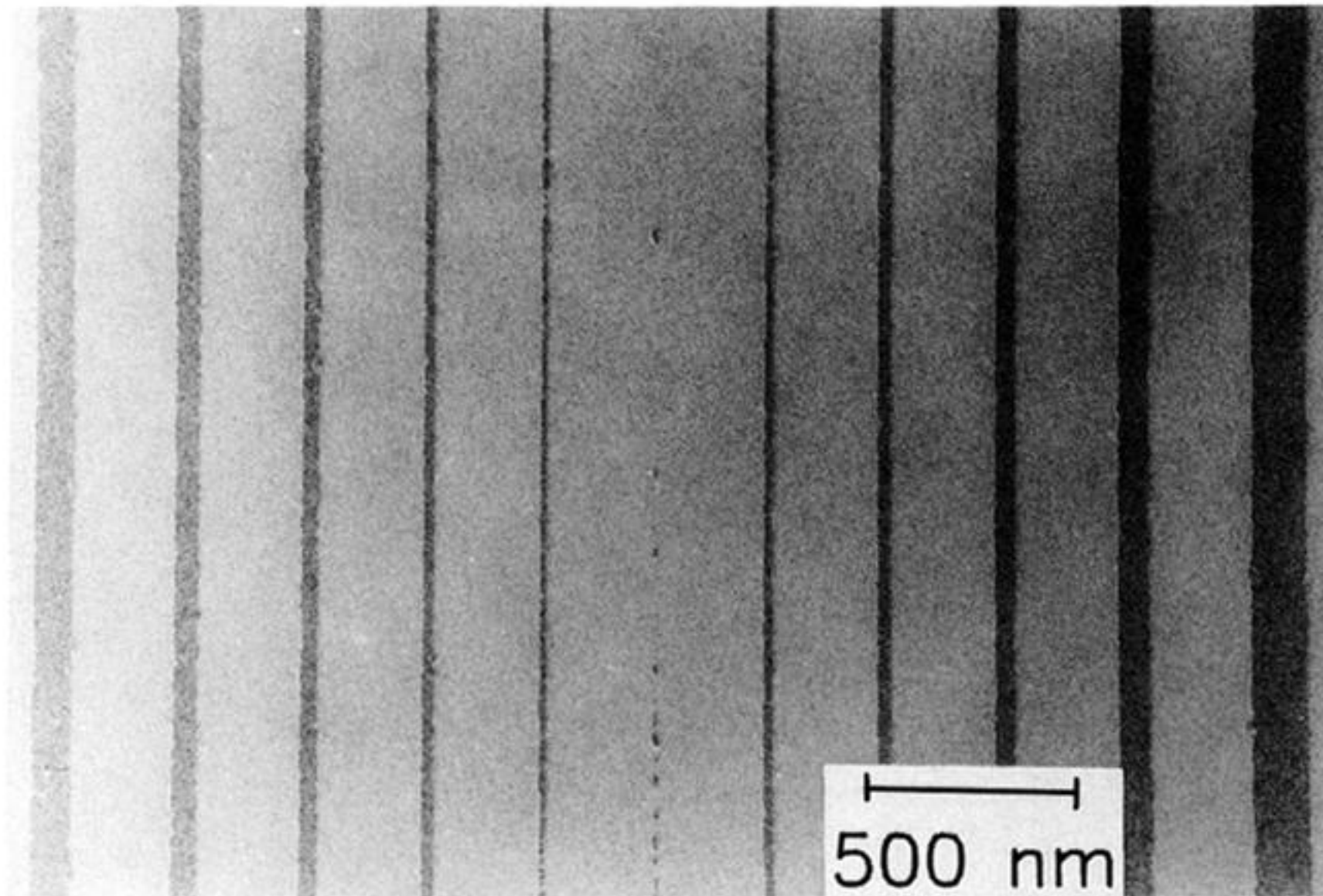


Figure 6. Au–Pd pattern demonstrating the resolution limit of lift-off with PMMA. The narrowest line, with a nominal width of 3.2 nm has not lifted off. The second narrowest line, with a nominal width of 6.4 nm is discontinuous. The 9.4 nm line is continuous to the extent that the metal film is continuous.

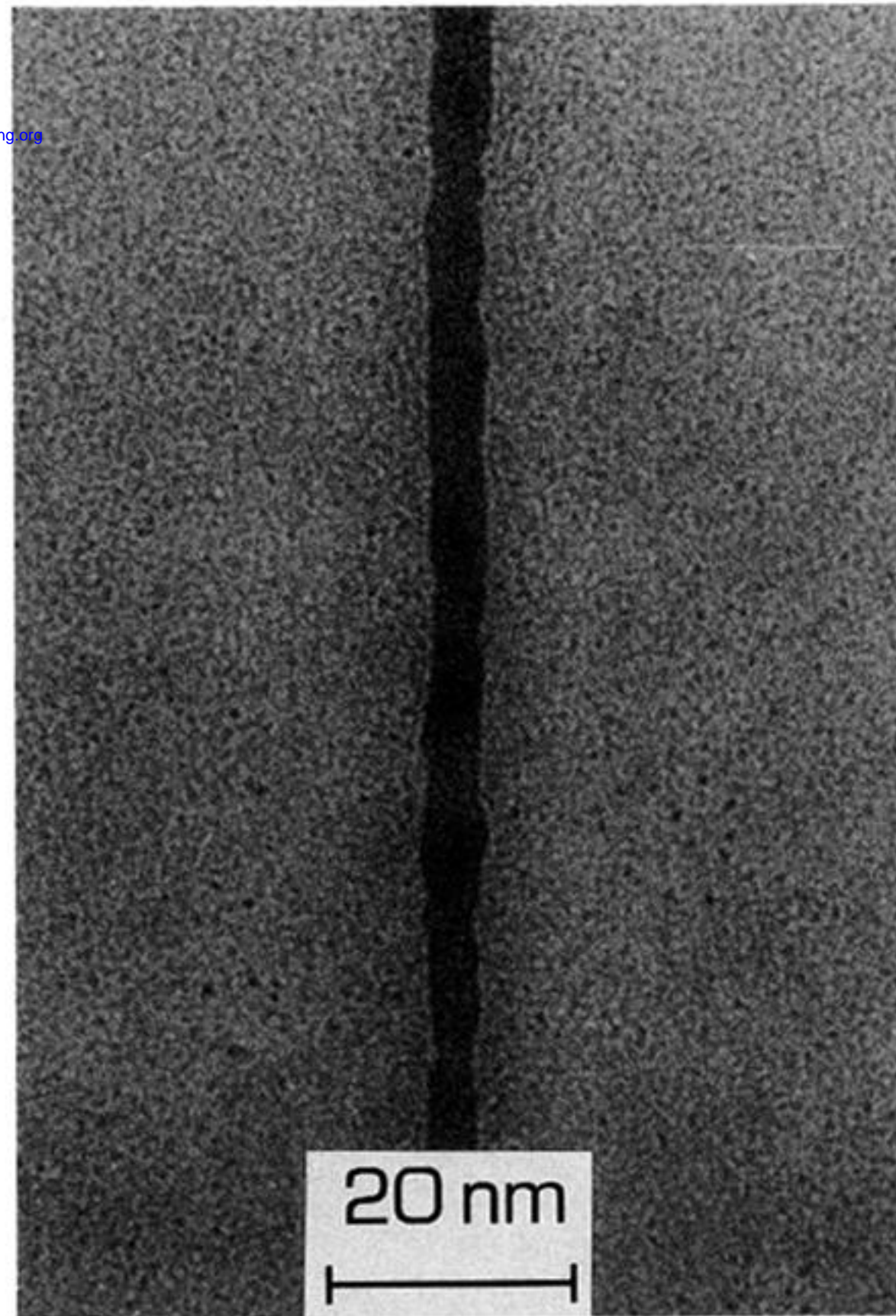


Figure 7. Au-Pd line with an average width of *ca.* 5 nm formed with vapour resist and ion milling.

Downloaded from [rsta.royalsocietypublishing.org](http://rsta.royalsocietypublishing.org)

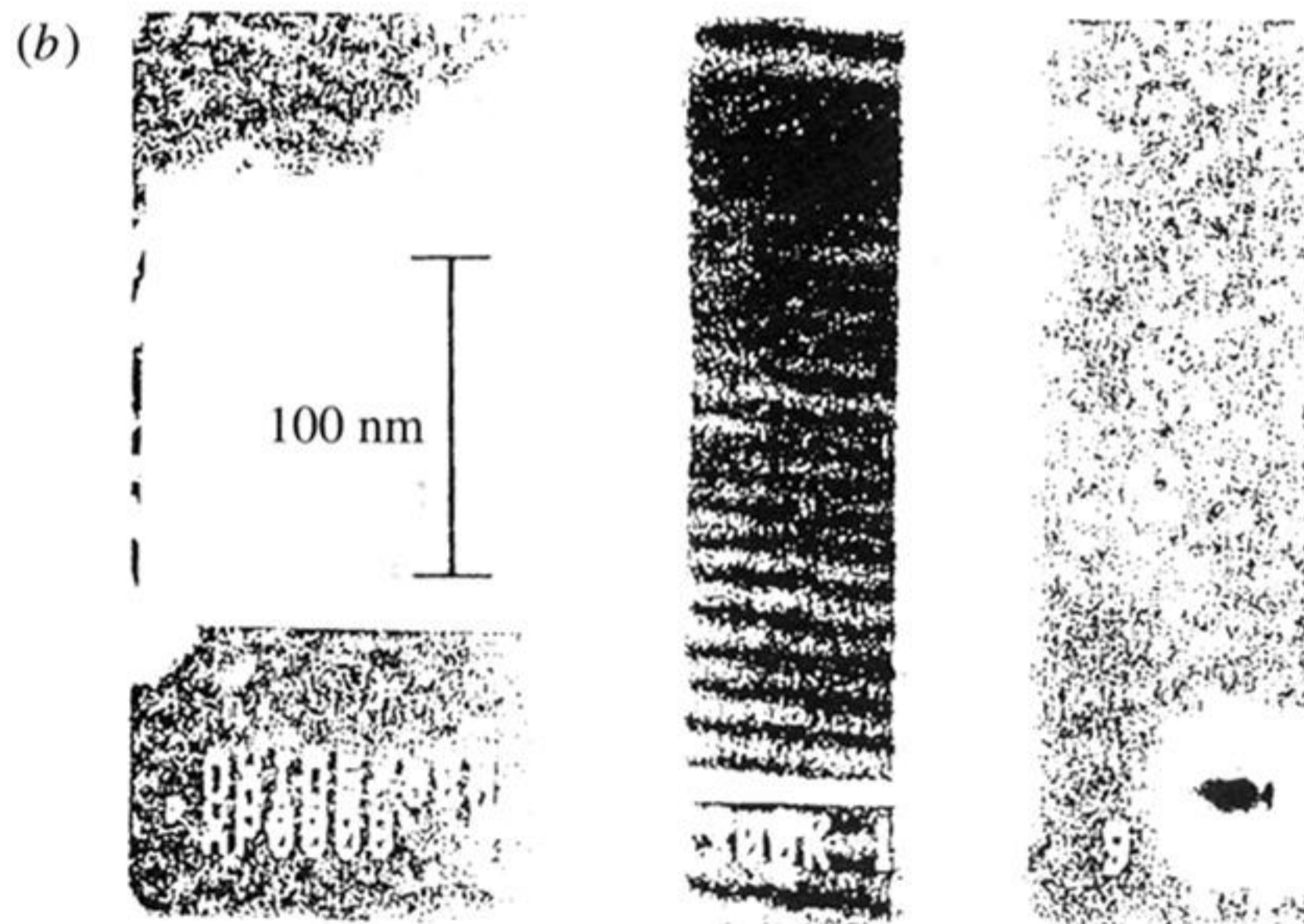
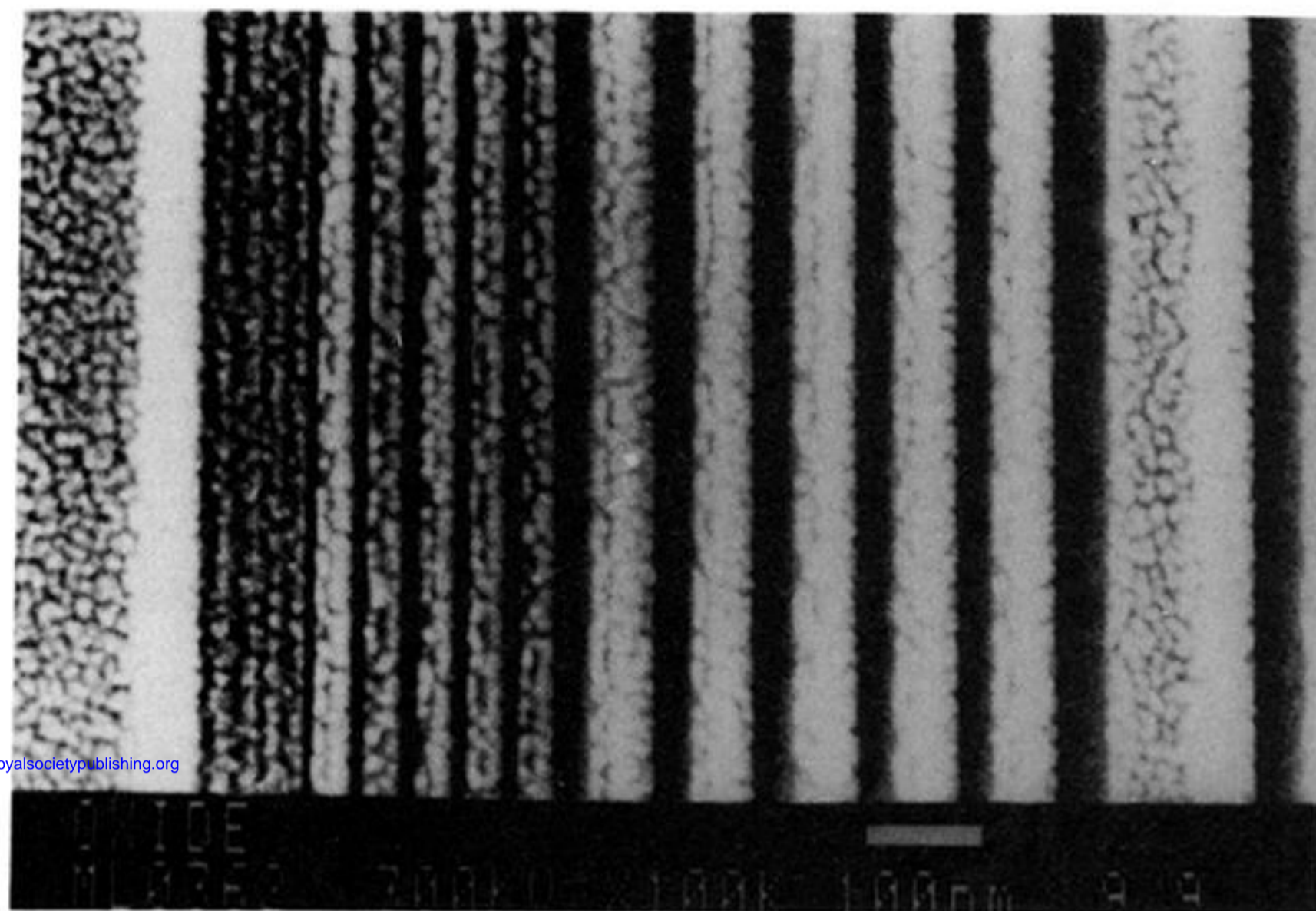


Figure 8. (a) Structures etched with HF-acid-based etches in  $\text{SiO}_2$  layers after e-beam irradiation. (b) High resolution test pattern in  $\text{SiO}_2$ ; 250 nm thick  $\text{SiO}_2$  layer is supported on 150 nm  $\text{Si}_3\text{N}_4$  membrane.

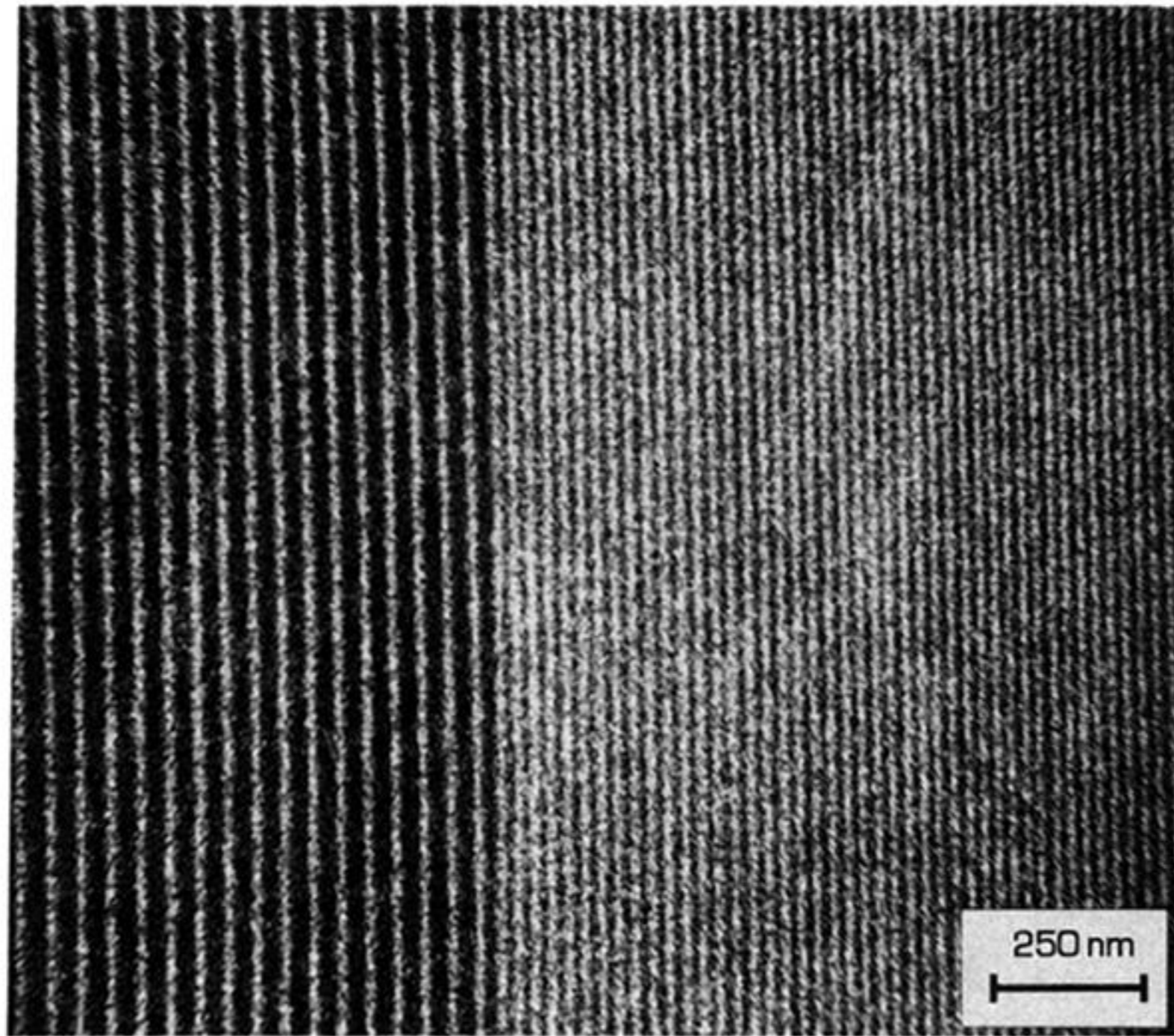
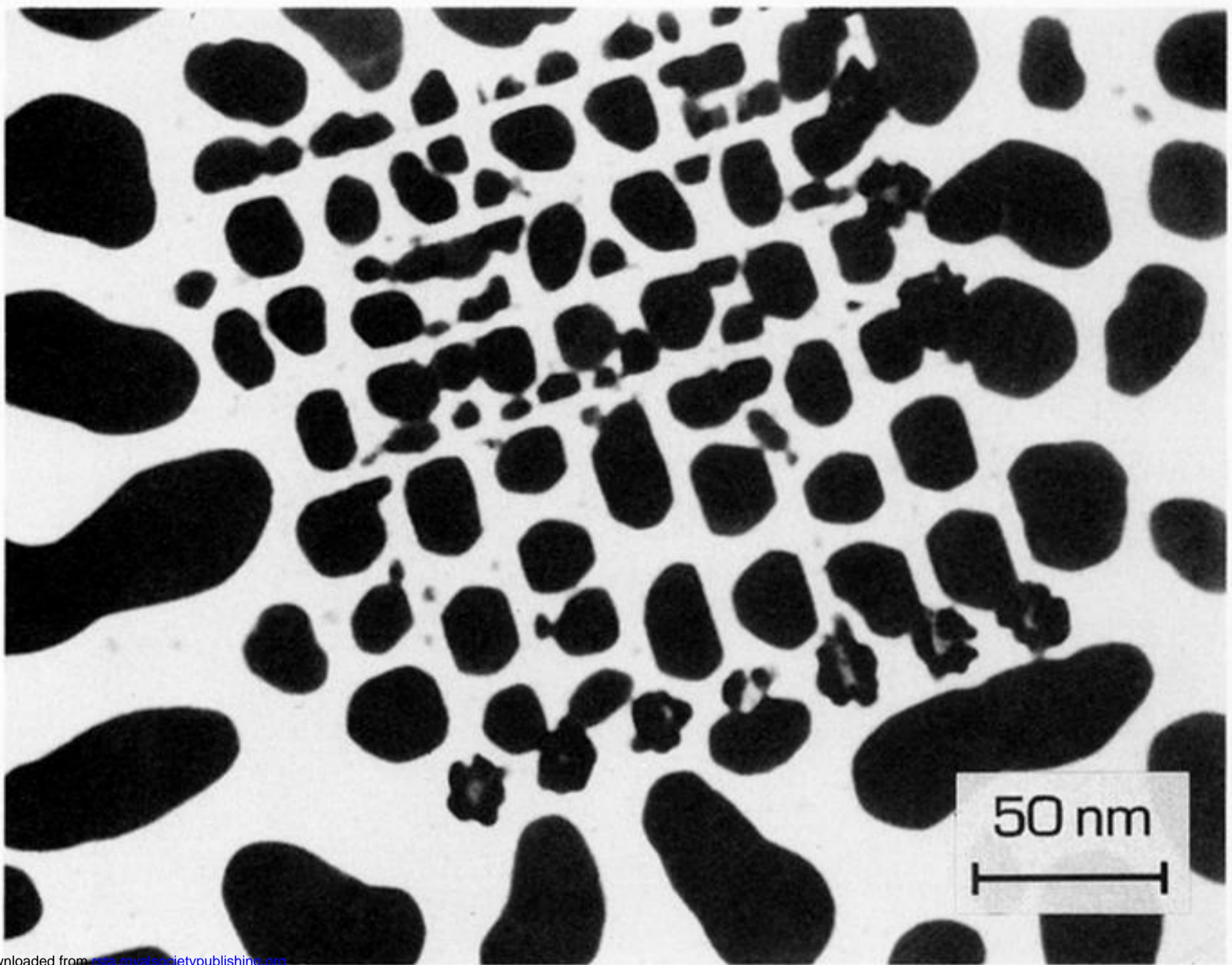


Figure 9. Lines written in a stack of Langmuir–Blodgett films using a 1 nm diameter, 50 kV electron beam (Broers *et al.* 1978).



Downloaded from [rsta.royalsocietypublishing.org](http://rsta.royalsocietypublishing.org)

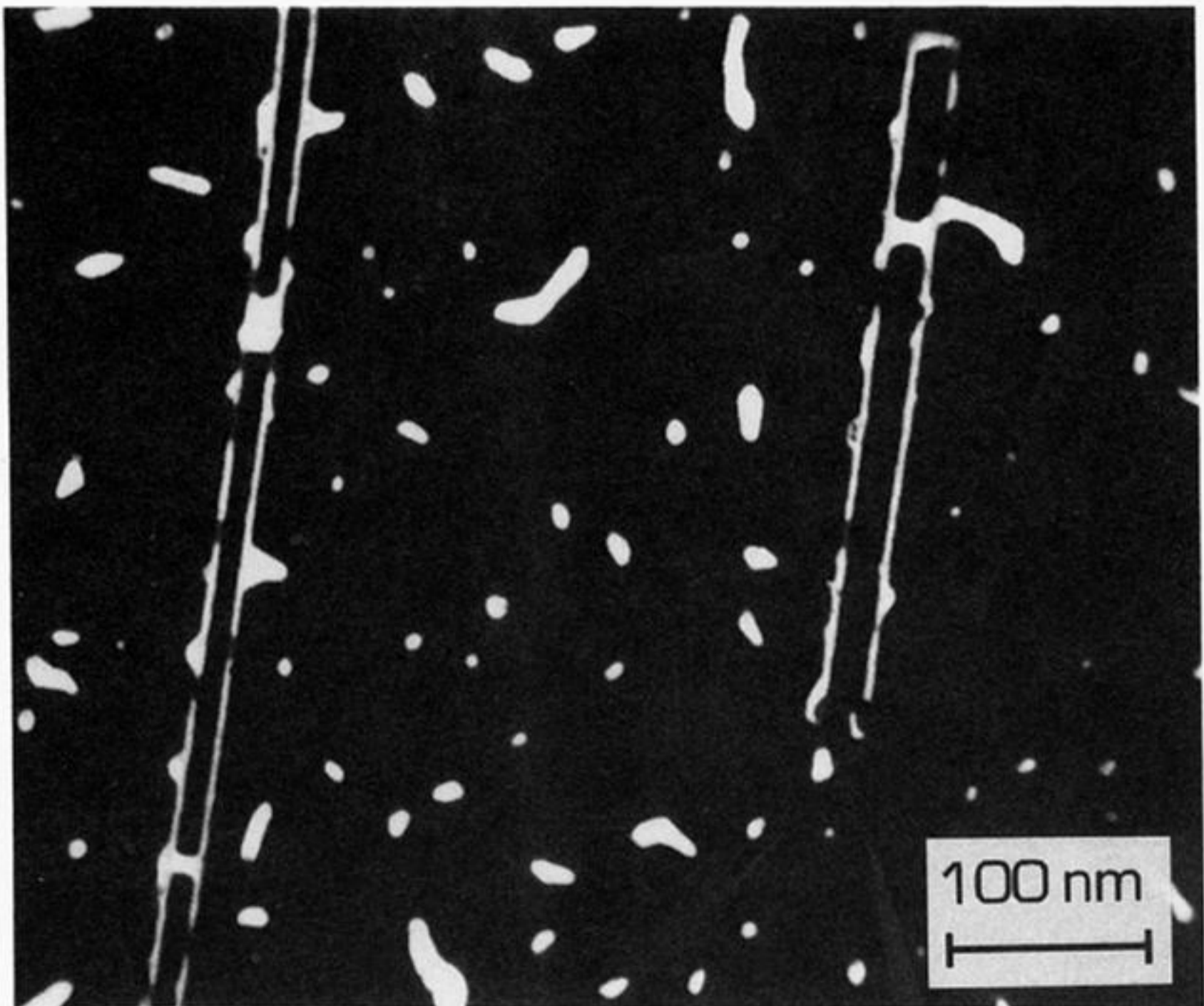


Figure 10. Patterns created by evaporating lead on top of vapour resist templates.